Journal of Materials Chemistry A

Enhancing the separation efficiency of C2H2/C2H4 mixture by a chromium Metal-Organic Framework fabricated via post-synthetic metalation

Journal:	*Journal of Materials Chemistry A*
Manuscript ID	TA-ART-06-2019-006913.R3
Article Type:	Paper
Date Submitted by the Author:	05-Dec-2019
Complete List of Authors:	Yu, Fan; Jianghan University, School of chemistry and environmental engineering Hu, Bing-Qian; Jianghan University, School of chemistry and environmental engineering Wang, Xiao-Ning; Luoyang Normal University, Zhao, Yu-Meng; Huazhong Univ Sci Li, Jialuo; Texas A&M University, Chemistry Li, Bao; Huazhong Univ Sci , ; huazhong university of science and technology Zhou, Hong-Cai; Texas A&M University, Chemistry

Journal Name

ARTICLE

Enhancing the separation efficiency of C_2H_2/C_2H_4 mixture by a chromium Metal-Organic Framework fabricated via post-synthetic metalation

Received 00th January 20xx,
Accepted 00th January 20xx

DOI: 10.1039/x0xx00000x

www.rsc.org/

Fan Yu[a,*], Bing-Qian Hu,[a] Xiao-Ning Wang[b], Yu-Meng Zhao[b], Jia-Luo Li[c], Bao Li*[,b] and Hong-Cai Zhou*[,c]

Abstract: Chromium Metal-Organic Frameworks (MOFs) had been well known for their stable porous framework, which is not fully explored due to the difficulty encountered in the synthesis process. In order to investigate the possibilities of Cr-MOFs as the separation materials towards C_2 guest molecules, a novel iron MOF had been constructed, which could be served as the scaffold to fabricate Cr-MOFs via post-synthetic metalation. The corresponding gas adsorption properties of two iso-structural MOFs had been systematically investigated, illustrating the potential separation ability of Cr-MOF with respects to CO_2/C_2H_2 and C_2H_2/C_2H_4. Furthermore, the real and feasible behaviors of gas separation for Cr-MOF had been verified by dynamic breakthrough experiments. Compared to the iso-structural Fe-MOF, the fabricated Cr-MOF not only improves the chemical stability, but also enhances the separation efficiency of C_2 gas molecules. The systematical investigation clearly manifests the important role of chromium ion towards the separation of gas molecules, and explore the other insight into fabricating the MOF-based separation materials.

Introduction

How to effectively and cost-efficiently carry out the purification of ethylene from C_2 mixtures is an important problem required the special attention.[1,2] In the current chemical industry, the separation process of cryogenic distillation for C_2 light hydrocarbons is a very energy-cost process, because of the close-boiling points and slight differences between the series of C_2 substances. Therefore, there are the related investigations shift to utilize porous materials to fulfill the non-thermally driven separation process, which is consistency with the development of modern cleaning concept.[3-6]

As one important type of the porous materials, Metal-Organic Frameworks (MOFs) have also received considerable attention due to their excellent structural-activity relationship, which exhibits the versatile applications in gas adsorption, heterogeneous catalyst, guest separation and luminescent sensing.[7-24] Importantly, MOFs-based separation materials have also made considerable research progress, which illustrates the vital role of open metal sites in enhancing the separation efficiency of C_2 molecules.[25-38] The subsequent research efforts have focused on how to effectively increase the number of open metal sites and separation efficiency. Most of the MOFs-based separation materials concentrate on the iron, cobalt and copper-based ones.[39-45] However, rare attention has focused on chromium-based MOFs since the unsolved difficulty in the effective construction of Cr-MOFs. Because of the strong connection mode caused by Cr(III) ion, Cr-MOFs usually exhibit the open metal sites, high chemical stability and large porous framework.[46-48] The corresponding structural advantages of Cr-MOFs ensure their potential as the separation materials towards C_2 matters, and the relevant systems are urgently needed to verify their separation performance. However, the effective construction of Cr-MOFs is still encountering the great challenge.

Recently, the preparation of Cr-MOFs by post-synthetic metalation (PSM) using Fe-MOFs as a template has proven to be of an effective strategy, which could be fulfilled in the moderate reaction environment.[49-50] Directed by the successful experience, in order to fabricate the proper Fe-parent, hexakis(4-formylphenoxy) cyclotriphosphazene (H_6L1), was chosen as the organic linkers for the following consideration: 1) The multi-connection mode and large size configuration of H_6L1 could ensure the formation of novel iron secondary building units(SBUs) since the classic iron-based SBU is trinuclear $[Fe^{III}_2Fe^{II}(O)(COO)_6]$; 2) The highly connection modes between Fe SBU and hexa-carboxyl ligands would facilitate the formation of parent framework with large porous surface area and open metal sites. More importantly, after the moderate PSM process, the fabricated Cr-MOFs could fully

[a] Key Laboratory of Optoelectronic Chemical Materials and Devices of Ministry of Education, School of Chemical and Environmental Engineering Jianghan University, Wuhan, 430056, PR China. E-mail: yufan0714@163.com.

[b] Key laboratory of Material Chemistry for Energy Conversion and Storage, School of Chemistry and Chemical Engineering, Huazhong University of Science and Technology, Wuhan, Hubei, 430074, PR China. E-mail: libao@hust.edu.cn.

[c] Department of Chemistry, Texas A&M University, College Station, Texas 77843-3255, United States. E-mail: zhou@chem.tamu.edu.

inherit the structural benefits exhibited by Fe-MOFs, and subsequently exhibit the potential application as gas separation materials. Herein, in accordance with our predesign, a new porous MOF, $[(Fe_3O)_2(H_2O)_4(HCOO)(L1)_2]_n$ (HUST-5, HUST = Huazhong University of Science and Technology), was constructed, which consists of the unprecedented [Fe_3O-COO-Fe_3O] SBU and stable porous framework. HUST-5 shows no any effect of gas separation towards C_2 series, but the post-synthetically fabricated Cr-MOF exhibit the corresponding separation effect. The systematic comparison of these two isomorphic materials clearly illustrates the important role of Cr ion in the aspect of C_2 separation, and explore the other insights into the construction of the highly-efficient separation materials. In addition, the detailed preparation, crystal structure and adsorption behaviors are reported below, along with the theoretical investigation on the guest-host interactions between different C_2 molecules and two isostructural clusters.

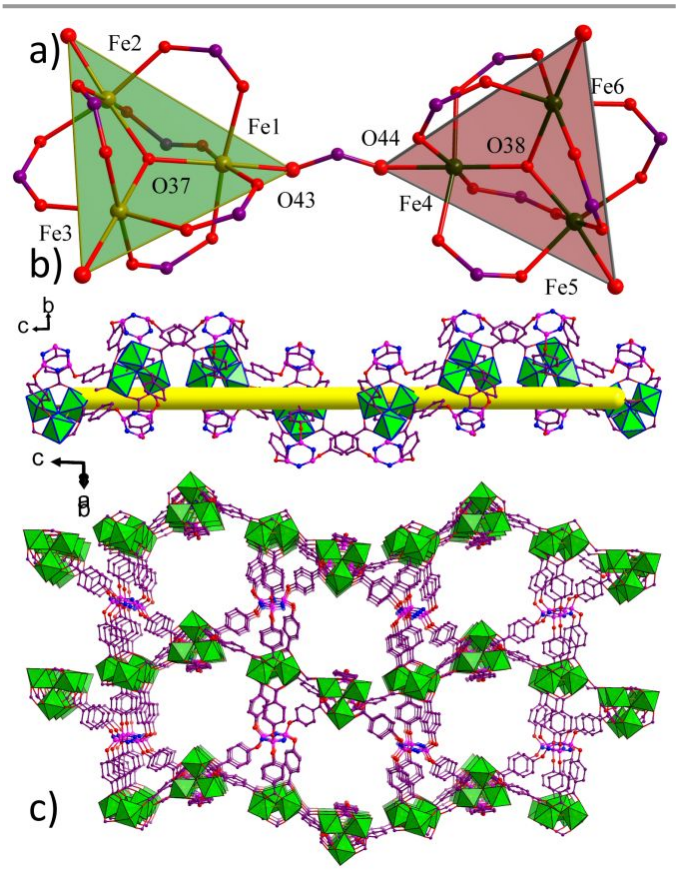

Figure 1. (a) Perspective view of the coordination environment of hexa-nuclear cluster, which consists of two tri-nuclear clusters bridged by formate anion; (b) Partial view of one dimensional arrangement of hepta-nuclear clusters ; (c) Partial view of two-dimensional channels of framework.

Results and discussion

Crystal Structure of Fe-MOF

The template Fe-MOF had been constructed by utilizing the typical [$Fe_3O(CH_3COO)_6$] inorganic cluster and hexa-carboxylate ligand under solvothermal condition. The polyhedron red crystal samples have been obtained at 150 ℃ for 3 days in DMF, which were directly utilized for the structural characterization, gas adsorption, preparing the isostructural Cr-MOF and other measurements. SCXRD data and selected structural parameters had been listed in Table S1-S2. SCXRD studies have found that HUST-5 crystallizes in monoclinic space group *C*2, whose asymmetric unit contains two Fe_3O clusters and two hexa-carboxylate ligands. All of the *syn-syn* acetate bridges in each tri-nuclear cluster have been substituted by the benzoate groups of four different ligands. Different to the isolated Fe_3O cluster in the reported MOFs, in HUST-5, two adjacent Fe_3O clusters are bind together via one formate anion to form the hexa-nuclear cluster, along with the dihedral angle of 72.58° (Figure 1). The other coordination sites of iron center are occupied by aqua molecules. Furthermore, the periphery of each hexa-nuclear cluster has been capped via six hexa-carboxylate ligands.

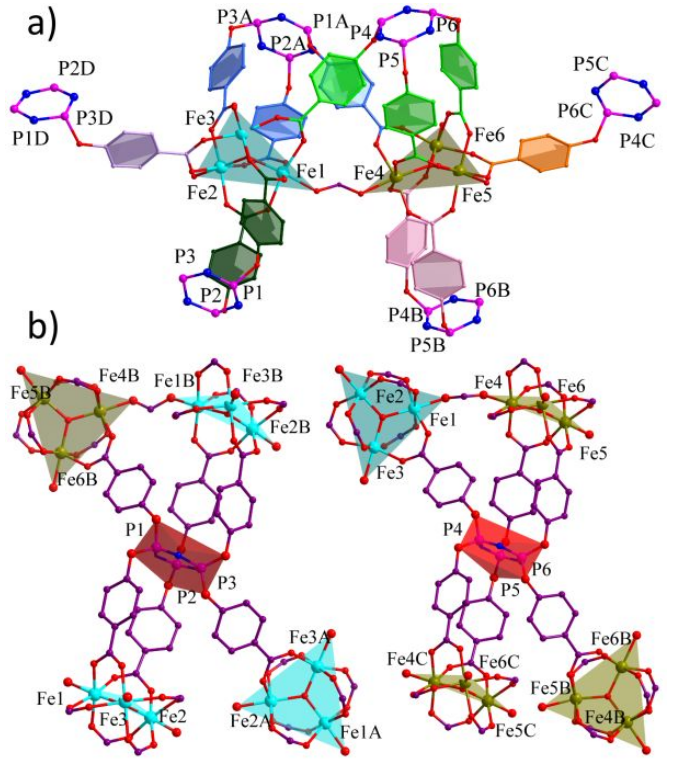

Figure 2. Perspective view of the coordination environment of metal cluster (a) and hexa-carboxylate ligands (b)

In HUST-5, there are two types of hexa-carboxylate ligands with the different connection modes (Figure 2). The substituted benzoate arms distribute equally on two sides of central ring. For each hexa-carboxylate ligand, three benzoate groups on two sides adapt different coordination modes to bind the same hexa-nuclear or two different hexa-nuclear clusters, along with the distorted $C_{carboxyl}$-$O_{substituted}$-$P_{central}$ angles ranged from 118.9 to 130.5°. The high connection mode between hexa-nuclear cluster and hexa-carboxylate ligands determines the fabrication of one dimensional SBU chain (Figure 1b), which must be the reason for the high stability of samples under vacuum conditions. Furthermore, each chain is

inter-connected by another four parallel 1D chains via the hexa-carboxylate backbones to construct the final 3D porous framework (Figure 3). Three dimensional porous channel was left in the packing structure (solvent accessible volume of 64.2% per unit cell calculated by the *PLATON* routine). If the separated trinuclear cluster and hexa-carboxylate ligands had been simplified as five- and four-connected modes, the topological structure of whole framework could be reduced as 4,5-c net with the point (Schläfli) symbol $\{3\cdot4\cdot7^2\cdot8^2\}\{3^2\cdot4^2\cdot7^5\cdot8\}$. The thermal and chemical stability of as-synthesized Fe-MOF had been examined via TGA and PXRD measurements (Figure S7-10), illustrating the stable porous structure under different strict conditions. Furthermore, the porous structure had been characterized by N_2 adsorption of activated Fe-MOF at 77 K, which exhibits the reversible type-I isotherm and gives the values of Langmuir surface area of 1020.3 $m^2\ g^{-1}$ (BET surface area of 802.2 $m^2\ g^{-1}$). The high connection mode between the novel metallic clusters and hexa-carboxylate ligands must be responsible for the stable porous structure in Fe-MOF.

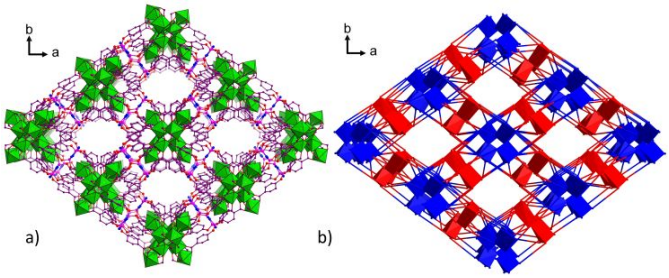

Figure 3. (a) Partial view of 3D porous structure of Fe-MOF HUST-5 along with *c*-axial direction; (b) Partial view of topological structure, blue and red polyhedrons represent the iron ions and hexa-carboxyl ligands.

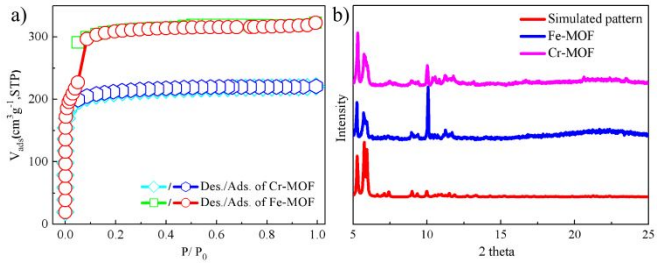

Figure 4. (a) N_2 sorption isotherms for activated HUST-5 (Fe-MOF) and HUST-6 (Cr-MOF) at 77K after vacuum-drying at 150 °C overnight. (b) XRD spectra of HUST-5 and HUST-6.

Post-synthetic Metalation of Fe-MOF to fabricate Cr-MOF

Due to the more stability of chromium MOF, the as-synthesized Fe-MOF (HUST-5) usually could serve as the metathesis template to prepare the isostructural Cr-MOF (HUST-6). Herein, when the red HUST-5 samples were immersed in acetone solution containing $CrCl_3\cdot6H_2O$ at 60°C for 3 days, obvious color-change of crystal samples to green sample could be observed. The crystallinity of single-crystal HUST-6 sample had been decreased in the process of metathesis, whilst the detailed structure could not be determined via SCXRD method. However, via the PXRD studies, the post-synthetic HUST-6 remains the isostructure compared to HUST-5 template (Figure 4). SEM studies manifest the uniform distribution of chromium ion in HUST-6, and no iron element could be detected (Figure 5). The stable porous framework of HUST-6 could be validated via N_2 adsorption at 77 K, which also exhibits the reversible type-I isotherm and gives the values of Langmuir surface area of 958.2 $m^2\ g^{-1}$ (BET surface area of 645.3 $m^2\ g^{-1}$). Compared to the porous characteristics of HUST-5, in HUST-6, the elimination of defects in the crystal sample during the process of metallic metathesis must be responsible for the decrease of porous surface area. During the soaking process, Cr^{3+} ions tends to repair the defects reserved in Fe-MOFs due to its proper coordination ability, resulting in a more regular crystal systems. During the Except for the change of porosity, the thermal and chemical stability of HUST-6 have been also improved due to the speciality of chromium ion(Figure S9). In addition, the defects of HUST-5 could be also decreased by the utilization of $FeCl_2$ salt with the modified synthesized method, which exhibits the similar adsorption behaviors to HUST-6 (Figure S23).

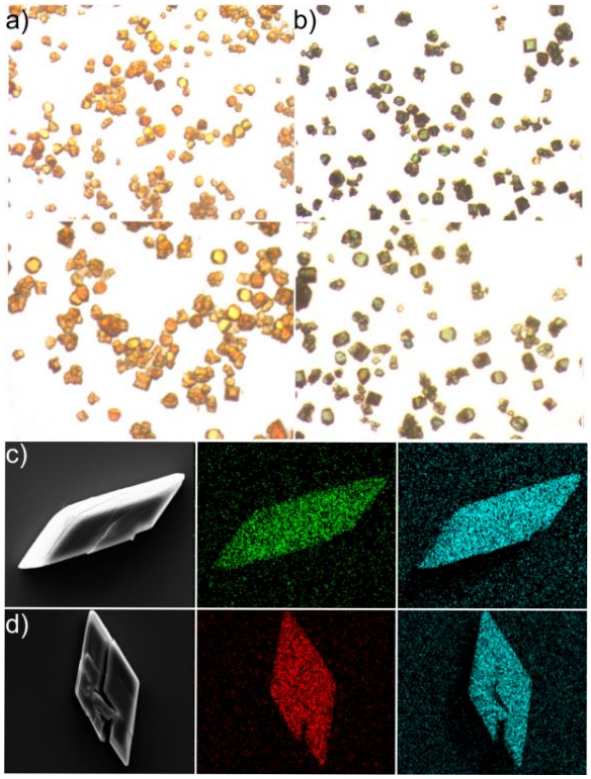

Figure 5. Images of HUST-5 (a) and HUST-6 (b); (c) SEM image of the as-prepared HUST-5 and EDX mapping image of Fe and P elements; (d) SEM image of HUST-6 obtained via metallic metathesis and EDX mapping image of Cr and P elements.

Gas separation ability of two isostructural MOFs

The permanent porosity and multiply interaction sites in these two isostructural MOFs encourages the further comparison of gas separation performances, in order to illustrate the important roles of iron and chromium ions on the separation for small gas molecules. Firstly, the adsorption amount for pure components of CO_2, CH_4, C_2H_6, C_2H_4 and C_2H_2 have been evaluated (Figure 6). Both of two isostructural MOF exhibit

adsorption capacities with the trend of C_2H_2>C_2H_4>CO_2>CH_4. With the consideration of the urgent requirement of the separation of C_2H_2/CO_2 and C_2H_2/C_2H_4 mixtures in industrial application, the separation performance of two MOFs had been comprehensively investigated. For these two MOFs, the largest adsorption amount of C_2H_2 with the uptake ratio of C_2H_2/C_2H_4 and C_2H_2/CO_2 in the range of 1.42 to 1.93 at 273 K, similar to the reported values for MOFs used in gas separation.[51-54] The adsorption amount of C_2H_2 for HUST-6 is much larger than HUST-5, indicating the much stronger interaction of HUST-6 compared to iron analogue. By virtue of virial equation, the isosteric heats of adsorption values (Q_{st}) for the zero loading of C_2H_2, C_2H_4, and CO_2 are calculated as 30.6, 29.2 and 29.4 kJ mol^{-1} for HUST-5, and 31.1, 30.2 and 28.3 kJ mol^{-1} for HUST-6, respectively (Figure 6). In term of the trend of adsorption enthalpies, these two isostructural MOFs exhibit the similar potential for thermodynamic separation of C_2H_2 from CO_2 and C_2H_4 mixtures.

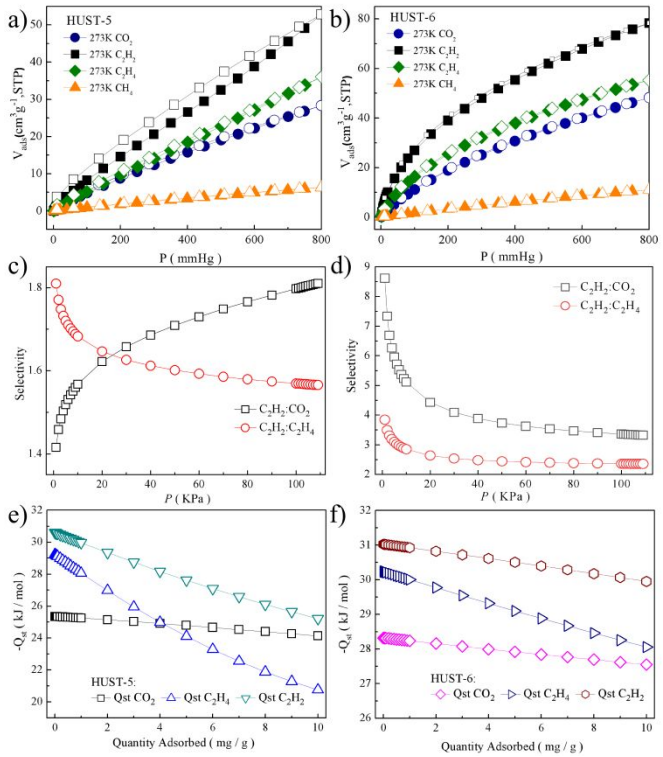

Figure 6. CO_2 , CH_4 and C_2H_x sorption isotherms for HUST-5 (Fe-MOF, a) and HUST-6 (Cr-MOF, b) at 273 K; IAST adsorption selectivity for HUST-5 (c) and HUST-6 (d) of equimolar C_2H_2/C_2H_x and C_2H_2/CO_2 mixtures; CO_2, C_2H_x isosteric heats of adsorption for HUST-5 (e) and HUST-6 (f).

Guided by the primary theoretical investigation, in order to further evaluate the gas separation performances of two MOFs, the adsorption selectivity for equivalent C_2H_2/C_2H_4 and C_2H_2/CO_2 binary mixtures have been simulated according to ideal adsorbed solution theory (IAST) (Figure 6). At 273K and initial pressure, the separation selectivity value of HUST-5 for the mixtures composed of equimolar binary C_2H_2/C_2H_4 and C_2H_2/CO_2 is 1.8 and 1.4. Under the same condition, the values calculated for HUST-6 reaches to 3.8 and 8.6, which are higher than those of the most promising MOFs for C_2H_2/C_2H_4 and/or C_2H_2/CO_2 separations, such as MOF-74-Fe (1.8 for C_2H_2/C_2H_4), NbU-3-MnFe (2.7 for C_2H_2/C_2H_4) and TIFSIX-2-Ni-i (6.2 for C_2H_2/CO_2). Clearly, the adsorption selectivity for C_2H_2/C_2H_4 and C_2H_2/CO_2 has been effectively enhanced due to the speciality of chromium ions.

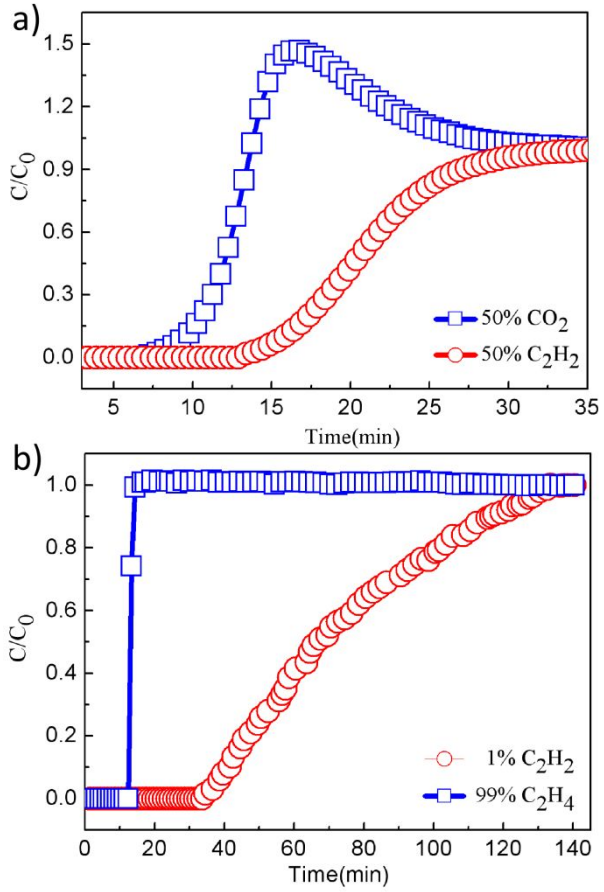

E

Figure 7. Breakthrough curves for CO_2/C_2H_2 (50/50) (a) and C_2H_2/C_2H_4 separations (1/99) (b) for HUST-6.

ncouraged by the above results of theoretical calculation, the dynamic breakthrough experiments had been further performed for the fully activated HUST-5 and HUST-6 towards the actual separation processes of C_2H_2/C_2H_4 (1:99, v/v) and C_2H_2/CO_2 (50:50, v/v) mixtures (Figure 7). The gas mixtures had been injected into a stainless column packed with the fully activated MOFs under the gas flow of 1.0mL/min at 290K. Under the same dynamic conditions, the highly efficient separations for HUST-6 could be obviously observed, compared to the negligible separation performances for HUST-5. For mixture of C_2H_2/C_2H_4 (1/99), the breakthrough time of C_2H_2 takes place approximately 33.5 minutes, indicating about 0.93 cm^3 of C_2H_2 being retained per gram of HUST-6. For C_2H_2/CO_2 (50/50, v/v), breakthrough of C_2H_2 for HUST-6 occurred after 13 min. The corresponding separation performance means that about 18.4 cm^3 of C_2H_2 has been captured, meaning about 63.0% of the amounts obtained from the single component adsorption isotherms (29.2 cm^3 g^{-1} at T = 298 K, $P(C_2H_2)$ = 0.5 bar). The systematic comparison clearly indicates chromium would play the important role in the field

of gas separation, and HUST-6 exhibit the promising potential application in C_2H_2 separation performance.

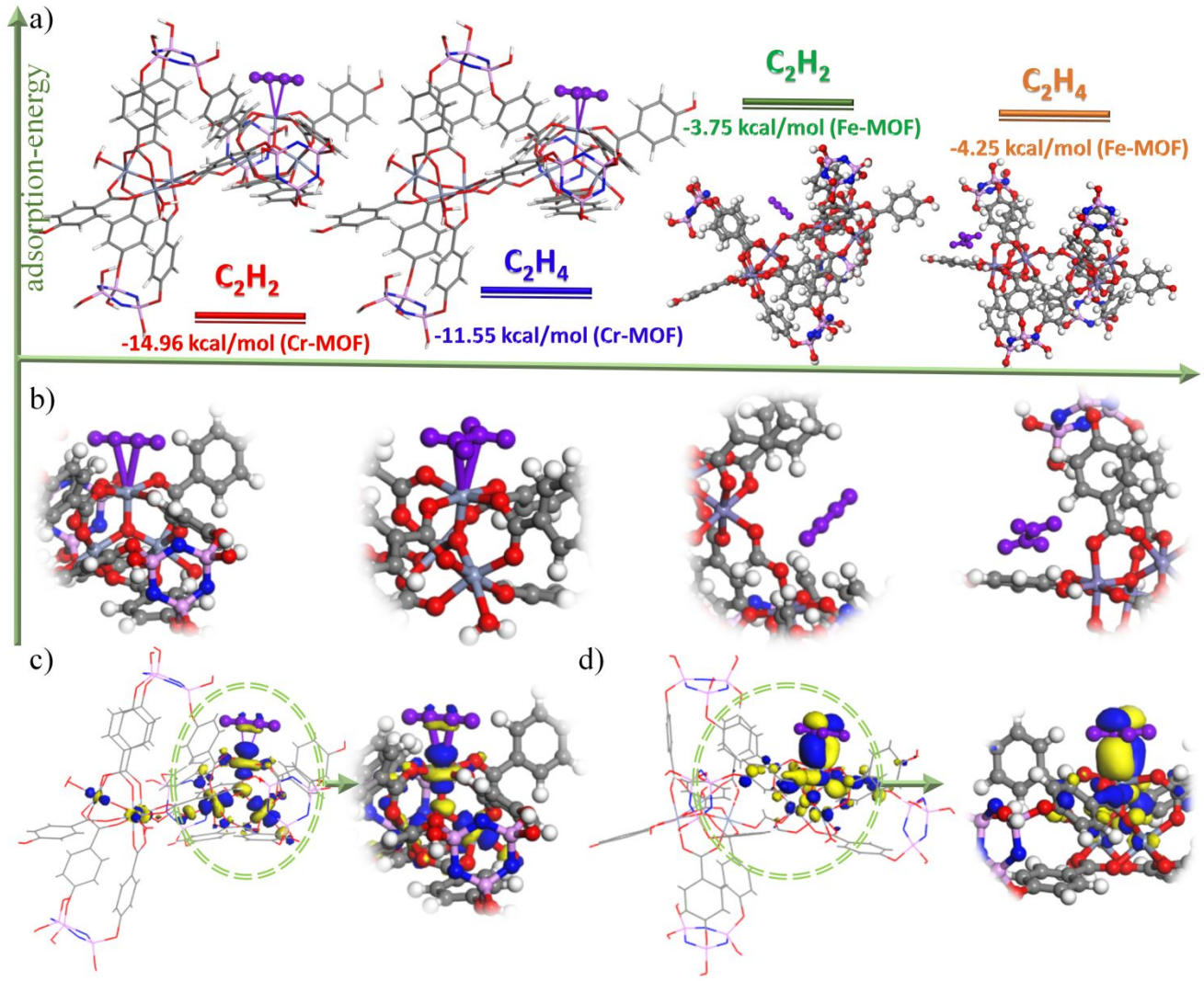

Figure 8. The view of the adsorption structure and adsorption energy of X/M-cluster (X= C_2H_2 and C_2H_4 , M = Fe and Cr) (a) along with the enlarged view of the adsorption sites (b); The view of frontier molecular orbitals Cr-cluster with C_2H_2(c) and C_2H_4(b).

The similar results could be also observed for the systems consisted of two isostructures of MIL-100(Fe) and its derivative MIL-100(Cr). No separation effect could be observed for Fe-based materials, but the moderate effect had been presented for Cr-based ones (Figure S26). Additionally, HUST-6 exhibits better performance compared to MIL-100(Cr), illustrating the important roles of porous structure and open metal sites on gas separation performance. This is also the key point we hope to explore in depth in the future. Herein, only the role of chromium ion had been illustrate with the systematic comparisons of two isostructures.

Theoretical calculation for two iso-structural MOFs

Compared to the iso-structures of HUST-5 and HUST-6, the elimination of defects might also supply the effect for improving the adsorption behaviors of different gas molecules. But the important role of open metal sites in different samples should be also fully considered for separation effect of C_2H_2 and C_2H_4. Therefore, theoretical calculation of Spin polarized Density functional theory had been carried out to illustrate the distinct separation performance for two iso-structural MOFs via the utilization of PBE/DNP theoretical level in the DMol^3 software[55-56]. In order to optimize the huge calculation amount in these two MOFs, the hexanuclear units of $(M_3O)_2(H_2O)_4(HCOO)(L2)_4$ (M = Fe, Cr) unit have been presented as the computational model. L2 means the simplified tetra-carboxyl ligands derived from the hexa-carboxyl ligand (Scheme S1). Geometrical optimization results reveal Cr-MOF keeps the same framework with Fe-MOF (see Figure S20), consistent with the observed PXRD result. For hexa-nuclear iron cluster, the dissociation energy between Fe ion and coordinated water molecule had been calculated as E_d = 1.21eV, giving the slight difference between the weak adsorption energy as E_a= -3.75 kcal/mol for C_2H_2 and -4.25 kcal/mol for C_2H_4. These calculated values for HUST-5 not only

mean the difficult in the activation process, but slight separation performance for C_2H_2/C_2H_4 mixture. Different to Fe cluster, the activation process is easier to manipulate with respect to the weak dissociation energy of E_d = 0.84 eV between the coordinated water molecules and Cr ions, illustrating the facile generation of open metal sites of one Cr ion in hexanuclear cluster (Figure S21). After the inspection of frontier molecular orbitals, it is manifested that LUMO mostly consist of 3d empty orbital of chromium(III) ion in the activated hexa-nuclear Cr system. Furthermore, the obvious difference between the adsorption-energy for C_2H_2 (E_a = -14.96 kcal/mol) and C_2H_4 (E_a = -11.55 kcal/mol) for the activated Cr cluster could illustrate the reason for the presentation of separation performance for HUST-6 (Figure 8). In addition, Hirshfeld charge population analysis shows that obvious electrons transfer from C_2 molecule to Cr ion (0.037e for C_2H_2 and 0.0014e for C_2H_4 , Figure 8c-d),which is also facile for the separation of C_2H_2/C_2H_4 mixture. Consequently, with the systematic comparison of iron and chromium-based separation substrates, the synergistic effect between open metal site of chromium ion and different C_2 molecules play the important role in the proper separation performance of C_2H_2/C_2H_4 mixture for HUST-6 compared to HUST-5.

Conclusions

In summary, a novel chromium MOF, HUST-6, had been constructed via the post-synthetic metalation of the iso-structural HUST-5 under the mild condition. The successful post-introduction of chromium ions not only effectively improve the chemical stability of the skeleton, but also enhance the corresponding parameters of the gas adsorption for series of C_2 molecules, illustrating the feasibility of HUST-6 as a promising separation material. Compared to the no effect of iso-structural HUST-5, the executive separation application of Cr-MOF towards CO_2/C_2H_2 and C_2H_2/C_2H_4 has been verified by dynamic Breakthrough experiment. With respect to the iso-structural framework in two frameworks, the origination of the distinct gas separation behaviors should be only ascribed to the different open metal sites of metal clusters. After the theoretical calculations, the different binding energy between the gas molecules and Cr clusters in HUST-6 had been presented, compared to the slight difference of Fe ones, adequately illustrate the important role of Cr ion in improving the performance of gas separation. The systematic comparison of two MOFs not only demonstrates the importance of Cr-MOF as a crystal engineering for building functional MOF materials, but also explores the other scientific insight into the MOFs-based separation materials!

Conflicts of interest

There are no conflicts to declare.

Acknowledgements

We must thank Dr. Gui-Lin Zhuang for theoretical calculation. This work was supported by the financial supports of National Science Foundation of China (21971078, 21471062), the Center for Gas Separations Relevant to Clean Energy Technologies, an Energy Frontier Research Center (EFRC) funded by the U.S. Department of Energy (DOE), Office of Science, and Office of Basic Energy Sciences (DESC0001015), Office of Fossil Energy, the National Energy Technology Laboratory (DE-FE0026472), and the Robert A. Welch Foundation through a Welch Endowed Chair to HJZ (A-0030), the Fundamental Research Funds for the Central Universities (2019kfyRCPY071, 2019kfyXKJC009), Hubei science and technology plan project (2019CFB769). We gratefully acknowledge the Analytical and Testing Center, Huazhong University of Science and Technology, for analysis and spectral measurements. We also thank the staffs from BL17B beamline of the National Center for Protein Sciences Shanghai (NCPSS) at Shanghai Synchrotron Radiation Facility, for assistance during data collection.

Notes and references

1 Y. Chen, Z. Qiao, H. Wu, D. Lv, R. Shi, Q. Xia, J. Zhou and Z. Li, *Chem. Eng. Sci.*, 2018, **175**, 110-117.
2 J. E. Bachman, Z. P. Smith, T. Li, T. Xu and J. R. Long, *Nat. Mater.*, 2016, **15**, 845.
3 A. Anastasaki, V. Nikolaou, Q. Zhang, J. Burns, S. R. Samanta, C. Waldron, A. J. Haddleton, R. McHale, D. Fox, V. Percec, P. Wilson and D. M. Haddleton, *J. Am. Chem. Soc.*, 2014, **136**, 1141-1149.
4 G. Centi, E. A. Quadrelli and S. Perathoner, *Energy Environ. Sci.*, 2013, **6**, 1711-1731.
5 Y. He, R. Krishna and B. Chen, *Energy Environ. Sci.*, 2012, **5**, 9107-9120.
6 A. Dhakshinamoorthy, Z. Li and H. Garcia, *Chem. Soc. Rev.*, 2018, **47**, 8134-8172.
7 X. Lian, Y. Fang, E. Joseph, Q. Wang, J. Li, S. Banerjee, C. Lollar, X. Wang and H. Zhou, *Chem. Soc. Rev.*, 2017, **46**, 3386-3401.
8 X. Yang, L. Chen, Y. Li, J. C. Rooke, C. Sanchez and B. Su, *Chem. Soc. Rev.*, 2017, **46**, 481-558.
9 R. Huang, Y. Wei, X. Dong, X. Wu, C. Du, S. Zang and T. C. W. Mak, *Nat. Chem.*, 2017, **9**, 689-697.
10 J. Xiao, L. Han, J. Luo, S. Yu and H. Jiang, *Angew. Chem. Int. Edit.*, 2018, **57**, 1103-1107.
11 B. Yan, *Acc. Chem. Rev.*, 2017, **50**, 2789-2798.
12 M. Wu and Y. Yang,*Adv. Mater.*, 2017, **29**,1606134.
13 J. Li, X. Wang, G. Zhao, C. Chen, Z. Chai, A. Alsaedi, T. Hayat and X. Wang, *Chem. Soc. Rev.*, 2018, **47**, 2322-2356.
14 Y. Chen, R. Zhang, L. Jiao and H. Jiang, *Coord. Chem. Rev.*, 2018, **362**, 1-23.
15 P. A. Kobielska, A. J. Howarth, O. K. Farha and S. Nayak, *Coord. Chem. Rev.*, 2018, **358**, 92-107.
16 L. Zhu, X. Liu, H. Jiang and L. Sun, *Chem. Rev.*, 2017, **117**, 8129-8176.
17 M. Cheng, C. Lai, Y. Liu, G. Zeng, D. Huang, C. Zhang, L. Qin, L. Hu, C. Zhou and W. Xiong, *Coord. Chem. Rev.*, 2018, **368**, 80-92.
18 N. S. Bobbitt, M. L. Mendonca, A. J. Howarth, T. Islamoglu, J. T. Hupp, O. K. Farha and R. Q. Snurr, *Chem. Soc. Rev.*, 2017, **46**, 3357-3385.
19 Q. Yang, Q. Xu and H. Jiang, *Chem. Soc. Rev.*, 2017, **46**, 4774-4808.

20 W. P. Lustig, S. Mukherjee, N. D. Rudd, A. V. Desai, J. Li and S. K. Ghosh, *Chem. Soc. Rev.*, 2017, **46**, 3242-3285.
21 Y. Huang, J. Liang, X. Wang and R. Cao, *Chem. Soc. Rev.*, 2017, **46**, 126-157.
22 E. A. Dolgopolova, A. M. Rice, C. R. Martin and N. B. Shustova, *Chem. Soc. Rev.*, 2018, **47**, 4710-4728.
23 T. Islamoglu, S. Goswami, Z. Li, A. J. Howarth, O. K. Farha and J. T. Hupp, *Acc. Chem. Rev.*, 2017, **50**, 805-813.
24 H. Wang, W. P. Lustig and J. Li, *Chem. Soc. Rev.*, 2018, **47**, 4729-4756.
25 J. Li, L. Jiang, S. Chen, A. Kirchon, B. Li, Y. Li and H. Zhou, *J. Am. Chem. Soc.*, 2019, **141**, 3807-3811.
26 N. B. Jayaratna, M. G. Cowan, D. Parasar, H. H. Funke, J. Reibenspies, P. K. Mykhailiuk, O. Artamonov, R. D. Noble and H. V. R. Dias, *Angew. Chem. Int. Edit.*, 2018, **57**, 16442-16446.
27 Bao, J. Wang, Z. Zhang, H. Xing, Q. Yang, Y. Yang, H. Wu, R. Krishna, W. Zhou, B. Chen and Q. Ren, *Angew. Chem. Int. Edit.*, 2018, **57**, 16020-16025.
28 H. Hao, Y. Zhao, D. Chen, J. Yu, K. Tan, S. Ma, Y. Chabal, Z. Zhang, J. Dou, Z. Xiao, G. Day, H. Zhou and T. Lu, *Angew. Chem. Int. Edit.*, 2018, **57**, 16067-16071.
29 L. Li, H. Wen, C. He, R. Lin, R. Krishna, H. Wu, W. Zhou, J. Li, B. Li and B. Chen, *Angew. Chem. Int. Edit.*, 2018, **57**, 15183-15188.
30 Y. Peng, T. Pham, P. Li, T. Wang, Y. Chen, K. Chen, K. A. Forrest, B. Space, P. Cheng, M. J. Zaworotko and Z. Zhang, *Angew. Chem. Int. Edit.*, 2018, **57**, 10971-10975.
31 J. Yan, B. Zhang and Z. Wang,*ACS Appl. Mater. Inter.*, 2018, **10**, 26618-26627.
32 C. B. Fan, L. L. Gong, L. Huang, F. Luo, R. Krishna, X. F. Yi, A. M. Zheng, L. Zhang, S. Z. Pu, X. F. Feng, M. B. Luo and G. C. Guo, *Angew. Chem. Int. Edit.*, 2017, **56**, 7900-7906.
33 M. Zhang, X. Xin, Z. Xiao, R. Wang, L. Zhanga and D. Sun, *J. Mater. Chem. A*, 2017, **5**, 1168-1175.
34 Y. Han, H. Zheng, K. Liu, H. Wang, H. Huang, L. Xie, L. Wang and J. Li, *ACS Appl. Mater. Inter.*, 2016, **8**, 23331-23337.
35 Y. Yan, M. Juricek, F. Coudert, N. A. Vermeulen, S. Grunder, A. Dailly, W. Lewis, A. J. Blake, J. F. Stoddart and M. Schroeder, *J. Am. Chem. Soc.*, 2016, **138**, 3371-3381.
36 J. Wang, R. Krishna, T. Yang and S. Deng, *J. Mater. Chem. A*, 2016, **4**, 13957-13966.
37 L. Li, R. Krishna, Y. Wang, J. Yang, X. Wang and J. Li, *J. Mater. Chem. A*, 2016, **4**, 751-755.
38 K. Liu, D. Ma, B. Li, Y. Li, K. Yao, Z. Zhang, Y. Han and Z. Shi, *J. Mater. Chem. A*, 2014, **2**, 15823-15828.
39 H. Wang, L. Hou, Y. Li, C. Jiang, Y. Wang and Z. Zhu,*ACS Appl. Mater. Inter.*, 2017, **9**, 17969-17976.
40 Q. Zhai, X. Bu, X. Zhao, D. Li and P. Feng, *Acc. Chem. Rev.*, 2017, **50**, 407-417.
41 T. L. Easun, F. Moreau, Y. Yan, S. Yang and M. Schroeder, *Chem. Soc. Rev.*, 2017, **46**, 239-274.
42 A. Cadiau, K. Adil, P. M. Bhatt, Y. Belmabkhout and M. Eddaoudi, *Science*, 2016, **353**, 137-140.
43 D. Xue, Y. Belmabkhout, O. Shekhah, H. Jiang, K. Adil, A. J. Cairns and M. Eddaoudi, *J. Am. Chem. Soc.*, 2015, **137**, 5034-5040.
44 Z. Zhang, Y. Zhao, Q. Gong, Z. Li and J. Li, *Chem. Commun.*, 2013, **49**, 653-661.
45 Y. He, R. Krishna and B. Chen, *Energy Environ. Sci.*, 2012, **5**, 9107-9120.
46 G. Ferey, C. Serre, C. Mellot-Draznieks, F. Millange, S. Surble, J. Dutour and I. Margiolaki, *Angew. Chem. Int. Edit.*, 2004, **43**, 6296-6301.
47 A. Sonnauer, F. Hoffmann, M. Froeba, L. Kienle, V. Duppel, M. Thommes, C. Serre, G. Ferey and N. Stock, *Angew. Chem. Int. Edit.*, 2009, **48**, 3791-3794.
48 G. Ferey, C. Mellot-Draznieks, C. Serre, F. Millange, J. Dutour, S. Surble and I. Margiolaki, *Science*, 2005, **309**, 2040-2042.
49 J. D. Evans, C. J. Sumby and C. J. Doonan, *Chem. Soc. Rev.*, 2014, **43**, 5933-5951.
50 J. Wang, Y. Zhang, M. Li, S. Yan, D. Li and X. Zhang, *Angew. Chem. Int. Ed.*, 2017, **56**, 6478-6482.
51 J. Li, L. Jiang, S. Chen, A. Kirchon, B. Li, Y. Li and H. Zhou, *J. Am. Chem. Soc.*, 2019, **141**, 3807-3811.
52 G. Jin, X. Niu, J. Wang, J. Ma, T. Hu and Y. Dong, *Chem. Mater.*, 2018, **30**, 7433-7437.
53 Z. Bao, J. Wang, Z. Zhang, H. Xing, Q. Yang, Y. Yang, H. Wu, R. Krishna, W. Zhou, B. Chen and Q. Ren, *Angew. Chem. Int. Ed.*, 2018, **57**, 16020-16025.
54 Z. Li, Y. Ye, Z. Yao, J. Guo, Q. Lin, J. Zhang, Z. Zhang, F. Wei and S. Xiang, *J. Mater. Chem. A*, 2018, **6**, 19681-19688.
55 B. Delley, *J. Chem. Phys.*, *1991*, **94**, 7245-7250.
56 B. Delley, *J. Chem. Phys.*, *2000*, **113**, 7756-7764.

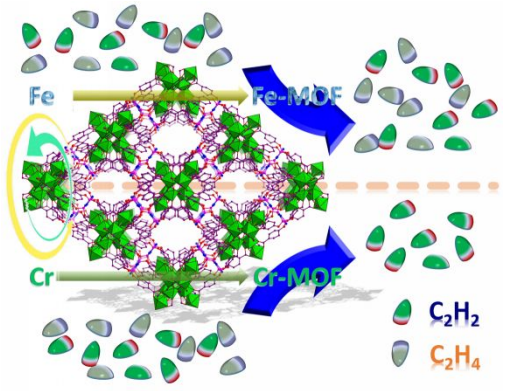

A new Cr Metal-Organic Framework had been fabricated via post-synthetic metalation, which exhibits the enhanced separation performance of C_2H_2/C_2H_4 compared to its template of isostructural Fe framework.